Detection of Pneumonia in Chest X-ray using Deep Learning Enabled Adaptive and Altruistic PSO-based Feature Extraction

K. Liharika
Department Of IT
Velagapudi Ramakrishna Siddhartha Engineering College
Vijayawada,India
liharikakola21@gmail.com

K. Bindu Sri
Department Of IT
Velagapudi Ramakrishna Siddhartha Engineering College
Vijayawada,India
bindukaturi2993@gmail.com

K. Harish
Information Technology
Velagapudi Ramakrishna Siddhartha Engineering College
Vijayawada,India
harishkoda72@gmail.com

C. Subba Reddy
Information Technology
Velagapudi Ramakrishna Siddhartha Engineering College
Vijayawada,India
chavvasubbareddy@gmail.com

2024 15th International Conference on Computing Communication and Networking Technologies (ICCCNT) | 979-8-3503-7024-9/24/$31.00 ©2024 IEEE | DOI: 10.1109/ICCCNT61001.2024.10724021

***Abstract*— Children die from pneumonia in many underprivileged areas around the world. The diagnosis of pneumonia in developing countries is still a difficult task, even with simple instruments available and medications available to treat it. Pneumonia can be identified in these nations using computer-aided diagnostic (CAD) technologies. We apply the ideas of deep learning and meta-heuristic algorithms to our pneumonia detection CAD system. In the first stage, we extracted the deep features by using the ResNet models. We performed feature extraction using various ResNet models—ResNet50, ResNet101, and ResNet152—to identify which model is better at extracting the features, and it can then be fine-tuned based on a target pneumonia dataset. After performing the feature selection procedure by particle swarm optimization, we modify the parameter using involvement of memory in adaptation and enrich it by developing agents that exhibit altruistic behavior We also consider adaptive and altruistic particle swarm optimization (AAPSO) for efficient feature selection and remove the non-informative features extracted by the ResNet model to improve the ability to detect pneumonia. In addition to ResNet models for feature extraction and AAPSO for feature selection, we applied the Support Vector Machine (SVM) algorithm for classification, as SVM is widely used for better classification and regression purposes.**

Keywords*— *Chest X-ray, Classification, Pneumonia, PSO, ResNet, SVM.

I. Introduction

According According to the statistics on pneumonia given by the World Health Organization (WHO), there were 7.40 million children who died due to pneumonia in 2019. Children are newly diagnosed with pneumonia in more than 90% of developing countries. In underprivileged countries like Africa, where resources are limited and there are no trained and experienced physicists, pneumonia diagnosis has become a difficult task. A dangerous illness called pneumonia damages the lungs by inflaming the alveoli, which results in serious breathing difficulties. The radiologist's diagnostic skill is the only factor that can accurately identify pneumonia from any of the aforementioned scans, yet the findings are still unreliable [1]. As a result, pneumonia can be detected using computer-aided diagnosis (CAD) systems. CAD systems are widely used to detect breast cancer, mammograms, and lung nodules. These are very expensive and take more time for analysis. Medical costs can be reduced, radiologists' efficiency can be improved, and the diagnosis and treatment of pneumonia can be accelerated using artificial intelligence (AI)-based diagnostics.

to

Despite substantial advancements in CAD systems for pneumonia detection, there are notable gaps in the literature. Existing studies often neglect the exploration of advanced hybrid optimization methods like adaptive and altruistic PSO (AAPSO) for feature selection, as proposed by [6], and they lack a comprehensive comparison of various ResNet architectures for feature extraction. Moreover, there is limited research on integrating deep CNNs for feature extraction, hybrid optimization algorithms for feature selection, and robust classifiers like SVM into a unified framework. Additionally, the trade-offs between model complexity and computational efficiency are frequently overlooked. Our study addresses these gaps by evaluating different ResNet architectures, implementing AAPSO for feature selection, and using SVM for classification, thereby enhancing the efficiency and effectiveness of pneumonia detection from X-rays of the chest.

II. Literature Review

Some recently proposed works on computer-aided diagnosis (CAD) systems for pneumonia detection are discussed below.

Gaobo Liang and Lixin Zheng [1] devised a method for diagnosing pediatric pneumonia by merging a deep residual network with transfer learning. They used the method of combining residual networks and dilated convolution. The accuracy of their test data was 96.7%. Several nonlinear models that have been trained to extract features induced by chest X-rays have been compared in a comparative analysis by Dimpy Varshini, Karthik Takral, Lucky Agarwal, Rahul Nijhawan, and Ankush Mittal. They presented these models with different classifiers to propose an ideal classifier for the same image classification. Throughout the classification process, they used a range of classifiers, such as Naive Bayes, Random Forest, K-Nearest Neighbors (KNN), and Support Vector Machines (SVM). The accuracy of kNN is 68.3%, Naive Bayes is 67.5%, and that of Random Forest is 67.3%. SVM provides the highest accuracy of 80% for classification [2]. Three classifiers—GoogleNet, Resnet18, and DenseNet-

121—have been proposed by Rohit Kundu, Ritacheta Das, Zong Woo Geem, Ram Sarka, and Gi-Tae Han as part of an ensemble framework to create a weighted ensemble. Testing the method on two publicly available pneumonia chest X-ray datasets yielded an accuracy percentage of 98.81% [3]. Using images from chest X-rays, YuDong Zhang, V. Rajinikanth, R. Pugalenthi, Nilanjan Dey, and N. Sri Madhava Raja have suggested a deep learning system (DLS) to diagnose lung problems. Using a softmax classifier, classic DLS like VGG16, VGG19, and ResNet50 are used for the initial classification experiments. The result shows that the VGG19 model with an RF classifier offers an accuracy of 95.70% [4]. For the identification of pneumonia, Patrik Szepesi and László Szilágyi presented a unique deep neural network architecture. At a dropout rate of 30%, the accuracy is 98.2% [5]. Rishav Pramanik, Sourodip Sarkar, and Ram Sarkar have presented an adaptive and altruistic PSO-based deep feature selection technique for pneumonia detection from chest X-rays [6]. We selected this research as our baseline project and improved accuracy by utilizing various ResNet models with SVM classifiers. An ensemble of fuzzy distance-based deep models has been presented by Rishav Pramanik, Momojit Biswas, Shibaprasad Sen, Luis Antonio de Souza Júnior, João Paulo Papa, and Ram Sarkar to aid in the detection of cervical cancer. Based on separate runs, Inception V3, MobileNet V2, and Inception ResNet V2 have achieved 95.30%, 93.92%, and 96.44%, respectively [7]. Weixiang Chen, Xiaoyu Han, Jian Wang, Yukun Cao, Xi Jia, Yuting Zheng, Jie Zhou, Wenjuan Zeng, Lin Wang, Heshui Shi, and Jianjiang Feng made the results of this study available [10]. The authors of the study referred to their system as a CT-based deep learning pathogen recognition system for pneumonia. Using a hybridization of PSO and the Gravitational Search Algorithm (GSA), Guha et al. [11] proposed handwritten script classification based on PSO and GSA. Memory-free GSAs are introduced to the concept of memory while updating their velocity. Although acceleration—a metric used in GSA to assess the degree of exploration and exploitation—remains memory-intensive, their suggested technique permits memory-free velocity. As a result, the algorithm's ability to strike a balance between exploration and exploitation may have certain problems. Bhatt, H., and Shah, M., have created an ensemble CNN model for the purpose of identifying pneumonia in chest X-ray pictures. High recall (99.23%) and an F1 score (88.56%) were attained in the study [12]. Sharma, S., & Guleria, K. (2023) developed a deep learning model that integrates VGG-16 with neural networks to identify pneumonia from chest X-ray images. On one dataset, the accuracy of the model was 92.15%, and on another, it was 95.4%. When compared against SVM, KNN, Random Forest, and Naïve Bayes, among other machine learning techniques, the model performed better in both datasets. This study demonstrates the effectiveness of VGG-16 with neural networks in accurately identifying pneumonia [13]. There is a recent proposal for a one-class detection technique by Zhang et al. [14]. A deep model was used for feature extraction, followed by modules for anomaly detection, confidence prediction, and anomaly fitting. Feature representation might have been improved with a fine-tuned network, and the final classification would have been improved as well.

III. Proposed Work

Detecting pneumonia using a deep model will be discussed in this section. To extract the best features, the chest X-ray picture samples are fed into a ResNet model that has already been trained. We then use AAPSO to select informative images and remove noise. We use SVM and KNN classifiers to determine the best accuracy.

A. Dataset Collection

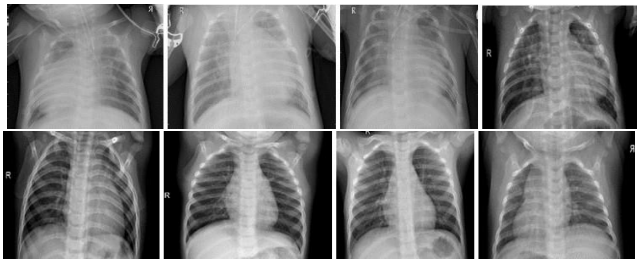

Fig. 1. The CXRs of both typical instances and people with pneumonia. These photos are from the Paul Mooney dataset. A typical row of CXR pictures is positioned above, while a row impacted by pneumonia is located below.

Our research used a dataset of pneumonia chest X-rays that was made available to the public. The dataset is available on the Kaggle website for convenient access. Table I and Fig. 1 contain descriptions of the photos in the dataset. There are two classes—normal and pneumonia—and three sets of training, testing, and validation data.

Table I. Description of images in the Chest X-ray dataset

Class	Setting	Samples
Normal	Train	1341
	Test	234
	Validation	8
Pneumonia	Train	3875
	Test	390
	Validation	8

B. Data Preprocessing

First, the photographs are improved and scaled using conventional techniques. Data techniques such as data augmentation and normalization enhance the dataset's quality and consistency. These processes ensure that images are standardized and optimized for subsequent analysis. By refining image quality and focusing on relevant features, preprocessing enhances the accuracy and reliability of pneumonia detection algorithms. Overall, meticulous preprocessing lays the solid groundwork for effective automated diagnostic systems in pulmonary healthcare.

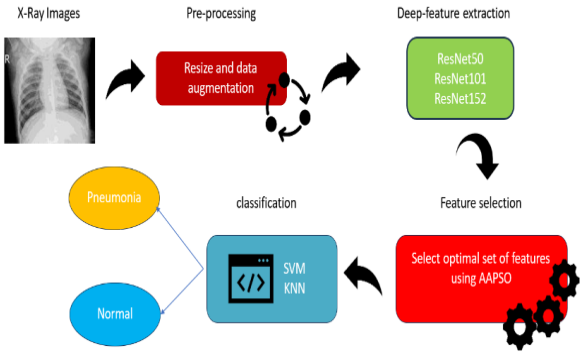

Fig. 2. A thorough rundown of our CXR-based deep model for pneumonia detection. The photos are first enlarged and resized using common procedures. The features are then extracted from these photos using the deep feature extractors ResNet50, ResNet101, and ResNet52. The most useful features are then chosen using the original AAPSO feature selector, and the features are supplied to the classifiers SVM and KNN to detect pneumonia.

C. Deep Feature Extraction

We considered various feature extractors like ResNet50, ResNet101, and ResNet152 and evaluated which extractor offers the best features by observing their accuracy.

We considered various feature extractors like ResNet50, ResNet101, and ResNet152 and evaluated which extractor offered the best features by observing their accuracy.
One of the most popular deep learning models is deep residual networks, or ResNet, as first described by [8]. There are several residual blocks that make up a ResNet architecture. Fig. 3 describes the architecture of the residual model. We observe that there are many layers from input to the last layer, and the very first thing that we can see from the figure is that there is a direct connection that bypasses some of the layers in between. The gradient-vanishing problem is a common problem in every deep-learning model. Deepening the network, the gradients become extremely small or vanish, which affects the learning of the model. These skipping layers help the model create a shortcut for the gradients to flow more easily during backpropagation. So, these skipping layers address the problem of vanishing gradients. Eq. 1 is frequently used to process a signal for a deep architecture, where w is the weight parameter and b is the bias. (bias being the difference between the output that the model predicts and the actual output). The input layer is altered via residual training in accordance with Eq. 2 [6].

$$F(x)=\text{ReLU}\,(w\,x+b) \tag{1}$$

$$H(x)=F(x)+x \tag{2}$$

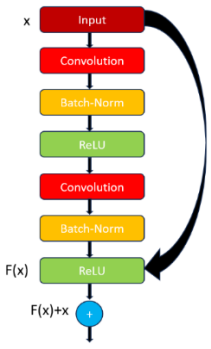

Fig. 3. An example of a residual block. Source: modified from [8].

D. Feature Selection

1.Particle Swarm Optimization

Kennedy and Eberhart introduced PSO, a low-cost, high-efficiency population optimization technique. Equations (3) and (4) provide a mathematical expression for it, where Pbest denotes a particle's individual best location and Gbest denotes the best position obtained by all particles combined in the swarm. Particles in PSO update both the best position found by every particle in the swarm (Gbest) and their own previous best positions (Pbest).

$$w_{ij}(t+1) = w_{ij}(t) + a1 * \left(Pbest_{ij} - z_{ij}(t)\right) + a2\left(Gbest_j - z_{ij}(t)\right) \tag{3}$$

$$z_{ij}(t+1) = z_{ij}(t) + w_{ij}(t+1) \tag{4}$$

In equation (3), the variables a1 and a2 represent two randomly selected values that fall within the range of 0 to 1. The velocity and position of the i^{th} particle in the j^{th} dimension are denoted by the words v_{ij} and x_{ij}, respectively. Gbest is the ideal global solution generated by the global best agent, whereas Pbest is the agent's best individual solution.

2.Adaptive PSO

The basic PSO method tends to trap populations near suboptimal solutions, hindering exploration and exploitation. Remaining search time affects the relative divergence of a solution, especially if using a maximum iteration cut-off. In the early rounds, a wider range of areas should be covered to ensure adequate investigation.

$$\frac{dS}{S} \propto dt \tag{5}$$

$$\frac{dS}{S} = c.dt \tag{6}$$

$$\int_{S_i}^{S_f} \frac{dS}{S} = c\int_{t_i}^{t_f} dt\text{h} \tag{7}$$

$$\log_e \frac{S_f}{S_i} = c.(t_f - t_i) \tag{8}$$

$$S_f = S_i.e^{c(t_f - t_i)} (\Delta S = S_i - S_f) \tag{9}$$

$$\frac{\Delta S}{S_i} = 1 - e^{c(t_f - t_i)} \tag{10}$$

$$w_{ij}(t+1) = b * w_{ij}(t) + a1 * \left(Pbest_{ij} - z_{ij}(t)\right) + a2 * (Gbest_{ij} - z_{ij}(t)) \tag{11}$$

Equation (5) provides the mathematical basis for the hypothesis. The variable dS quantifies relative divergence from the current solution, where S is the current solution and dS represents its change. dt represents a change in time.
Equation (6) introduces an equality term using a proportionality constant c. For experimental purposes, c is typically set to 1 and integrated within limits, considering the algorithm's start and end time. The first solution is denoted by cap S sub i, while the last solution is denoted by cap S sub f. In equation (8), pertinent limits are applied, and the final value is derived in equation (10) after some adjustments demonstrated in equation (9).

3.Trnasfer Function And Fitness Value

PSO is designed for optimizing continuous values. The standard S-shaped transfer function is used in feature selection. The process of binarizing continuous values

involves selecting a random number between σ(x) and the original values.

$$\sigma(x) = \frac{1}{1+e^{-x}} \quad (12)$$

$$(\sigma(x)) = \begin{cases} 1 \; if \; \sigma(x) \geq rand \\ 0 \; if \; \sigma(x) < rand \end{cases} \quad (13)$$

$$Fitness = \alpha \times a + (1-\alpha) \times f \quad (14)$$

To evaluate solutions, use formula (14) to calculate the fitness value. It includes accuracy 'A', feature ratio 'f', and hyperparameter 'α'.

PSO is a feature selection algorithm that reduces the feature dimension based on velocities. However, it fails to consider generational memory, which can cause the algorithm to stray outside the search space's informative region. To solve this issue, we can minimize the fitness value change for each repetition. Additionally, when selecting a feature that is not particularly clear, we need to evaluate it again in the search area. This approach can help agents that are not well-suited move to the selected feature subset.

4.Altruistic PSO

Selfless concern for others is the hallmark of altruism, and it may be seen in both humans and certain animals. We rank agents according on how their fitness scores have changed from the previous iteration in order to apply this idea to PSO. When significant changes occur, we let the agent to choose its best choice and then take use of it to produce more thorough search results. Elite agents, or the top k% of agents, are permitted to converge to the best answer. Regarding the agents themselves, the top half matches the worst with the worst, the second-best with the second-worst, and so on in order to benefit the bottom half.

Fig. 4. Flow digram of the model

5. Hyperparameters

In our research, we employed a Particle Swarm Optimization (PSO) algorithm with several key hyperparameters: the population size was set to 30 agents, with a maximum of 100 iterations. The fitness calculation assigned a weight of 0.98 to accuracy, utilizing a sigmoid transfer function shape. For classification and validation, we experimented with various train/test split ratios of 0.2, 0.3, 0.4, and 0.5, as well as 5-fold and 10-fold cross-validation. During the deep learning training phase, we tested multiple batch sizes of 16, 32, 64, and 128, over 10 epochs, and with learning rates of 0.01, 0.001, and 0.0001. In addition, we used a momentum of 0.9 to change the learning rate every 5 epochs. For normalization, a mean of [0.485, 0.456, 0.406] and a standard deviation of [0.229, 0.224, 0.225] were employed. Training was conducted on a GPU if available, otherwise on a CPU, with data loading configurations set as follows: 32 and 1 batch, respectively, were used for training and validation, with 4 workers for parallel data loading. These hyperparameters were critical for the successful implementation and replication of our machine learning experiments.

IV. Results

A. Analysing Results For ResNet Models

We considered various feature extractors like ResNet50, ResNet101, and ResNet152 and evaluated which extractor offers the best features by observing their accuracy.

Table II. Model accuracy and SVM accuracies of ResNet models

ResNet model	Model accuracy	SVM accuracy
ResNet50	93.75	95.6
ResNet101	93.45	94
ResNet152	93.33	95.2

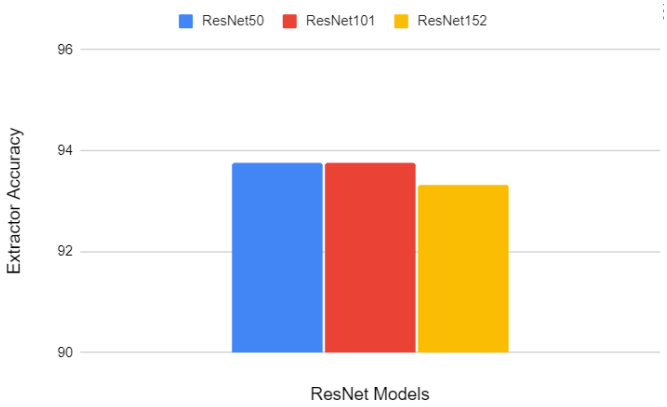

Fig. 5. Plot showing the accuracies of ResNet models.

Table III. Comparison of various algorithms

Model	Accuracy	PSO	Altruistic-PSO	AAPSO
DenseNet121	96.12	97.44	97.42	97.35
GoogleNet	95.55	96.67	97.09	97.35
VGG16	94.70	97.01	97.18	97.61
ModelNetV2	95.52	95.73	96.24	96.50
ResNet50	93.75	95.6	95.6	95.6

ResNet101	93.45	94	94	94
ResNet152	93.33	95.2	95.2	95.2

B. Performance of SVM Classifier

AAPSO was utilized to choose pertinent photos for SVM classification, and resNet50 was employed to extract features. Testing was done using several batch sizes and learning rates. The results showed that a batch size of 16 and a learning rate of 0.0001 produced the best accuracy, with accuracies of 88.8%, 94%, and 95.6% at learning rates of 0.01, 0.001, and 0.0001, respectively.

Table VI. Performance metrics achieved after applying SVM with learning rate of 0.0001

Batch Size	Test Size	Accuracy	Precision	Recall	F1
16	40	95.6	98.09	95.06	96.55
	30	92.55	94.55	92.86	93.69
	20	95.2	93.9	98.65	96.05
	5-fold	92.94	93.19	95.9	94.46
	10-fold	93.27	93.39	96.15	94.7
32	40	94	95.33	94.7	95.02
	30	93.62	96.55	93.33	94.92
	20	92	93.42	93.42	93.42
	5-fold	94.32	94.32	96.66	95.44
	10-fold	90.2	95.62	96.92	96.2
64	40	95.2	95.6	96.82	96.2
	30	95.21	95.12	97.5	96.3
	20	92.8	95.18	98.59	93.96
	5-fold	95.19	95.16	96.66	96.23
	10-fold	93.91	94.55	96.92	85.4
128	40	95.6	93.87	99.35	96.53
	30	93.09	93.75	96	94.86
	20	93.6	95.18	95.18	95.18
	5-fold	95.51	95.57	97.43	96.46
	10-fold	94.39	94.37	96.92	96.05

Fig. 6. Plot displaying the varied SVM accuracy values for various batch sizes and learning rates at 0.0001.

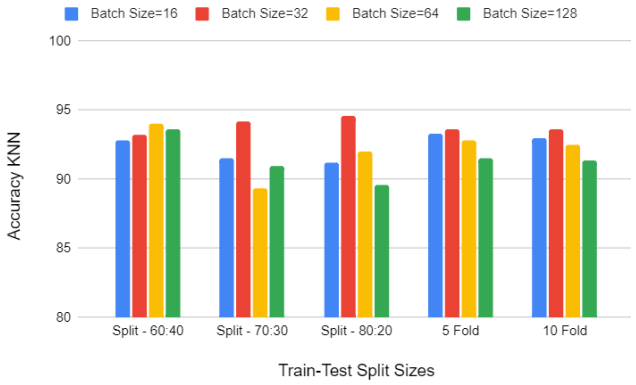

Fig. 7. Plot displaying the varied KNN accuracies at several batch sizes and learning rates at 0.0001.

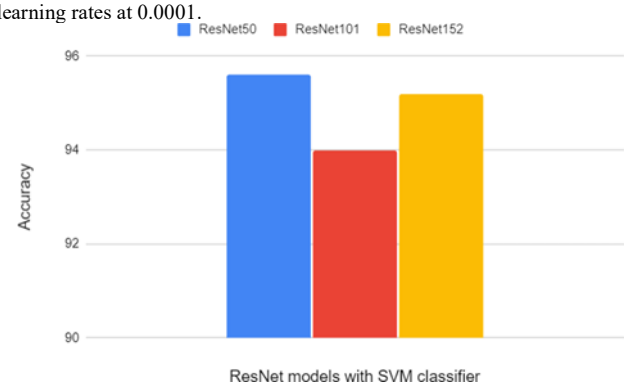

Fig. 8. Plot showing the accuracies of ResNet models with SVM classification

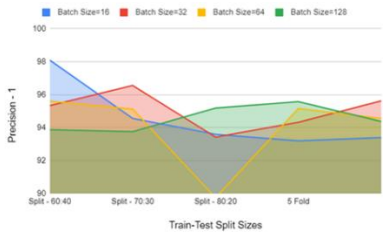

Fig. 9. Area displaying the different precision rates for SVM at 0.0001 learning rate and batch sizes

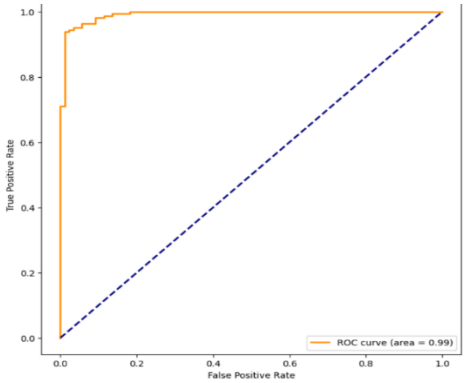

Fig. 10. ROC curves after feature selection with a batch size of 16 and a learning rate of 0.0001 for the Normal and Pneumonia classes.

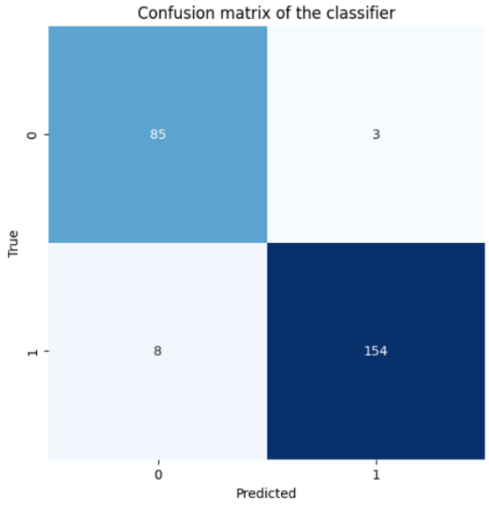

Fig. 11. Confusion matrix of the experiment after feature selection with a 16-bath size and a learning rate of 0.0001.

V. Conclusion

We provide a work-in-progress artificial intelligence-based pneumonia detection approach based on chest X-ray images. At first, we considered the pre-trained models ResNet50, ResNet101, and ResNet150 well-trained on a large ImageNet dataset for extracting features from the CXRs. We tested all three ResNet models and checked the results to choose which model had the highest accuracy. We selected ResNet50 for feature extraction as it provided the highest accuracy compared to other models. ResNet50 outperformed ResNet101 and ResNet150 in our study primarily due to its balanced architecture, which provides sufficient depth for feature extraction while maintaining computational efficiency. Deeper networks like ResNet101 and ResNet150, though capable of capturing more complex patterns, often suffer from overfitting, particularly with smaller datasets. Moreover, the increased number of layers in these deeper models results in higher computational costs without proportional gains in accuracy. Therefore, ResNet50's optimal complexity makes it more effective for our pneumonia detection task.

We then fine-tuned the ResNet50 model with our target chest X-ray dataset. The features extracted by the ResNet50 model are fed to the original AAPSO proposed by [6] to select appropriate features and finally classify the system using the SVM classifier. Using ResNet50 for feature extraction, AAPSO for feature selection, and SVM for classification, we assessed the model's performance at various batch sizes with learning rates of 0.01, 0.001, and 0.0001 across different data splits. At a learning rate of 0.01, the accuracy ranged from approximately 81.91% to 87.19%, with precision and recall showing moderate values around 75.41% to 91.19% and 70.1% to 95.42% respectively. The F1 scores for this learning rate varied from 73.02% to 90.35%. Performance measures improved when the learning rates were lowered to 0.001, with recall rising from 83.82% to 96.92%, accuracy from 90.22% to 94.39%, and precision from 86.75% to 92.47%. The F1 scores for this rate ranged from 79.67% to 94.46%. The greatest results were obtained with a learning rate of 0.0001, where recall ranged from 88.47% to 97.43%, accuracy from 90.2% to 95.51%, and precision from 92.99% to 95.62%. The F1 scores were also the highest, ranging from 90.26% to 96.46%. Additionally, larger batch sizes (64 and 128) generally yielded better performance, and higher data splits (70:30, 80:20) showed improved metrics across all learning rates. These observations suggest that the optimal model configuration includes a learning rate of 0.0001 with larger batch sizes and higher data splits for achieving the best results.

References

[1] liang, g. (2019, june 25). elsevier. A transfer learning method with deep residual network for pediatric pneumonia diagnosis, Comput. Methods Programs Biomed. (2020), 9.

[2] Dimpy Varshini, karthik takral, lucky agarwal, rahul nijhawan, & ankush mittal. (n.d.). Pneumonia Detection Using CNN based Feature Extraction. IEEE, 7.

[3] Rohit Kundu, Ritacheta Das, Zong Woo Geem, Ram Sarka, & Gi-Tae Han. (2021, 9 7). Pneumonia detection in chest X-ray images using an ensemble of deep learning models.

[4] YuDong Zhang, V. Rajinikanth, , R. Pugalenthi, Nilanjan Dey, & N. Sri Madhava Raja. (2021, march). elsevier. Customized VGG19 Architecture for Pneumonia Detection in Chest X-Rays.

[5] Patrik Szepesi, & , László Szilágyi. (2022, july 22). elsevier. Detection of pneumonia using convolutional neural networks and deep learning.

[6] Rishav Pramanik, Sourodip Sarkar, & Ram Sarkar. (2022, July 29). ELSEVIER. An adaptive and altruistic PSO-based feature selection method for Pneumonia detection from Chest X-rays, 14

[7] Rishav Pramanik, Momojit Biswas, Shibaprasad Sen, Luis Antonio de Souza Júnior, João Paulo Papa, & Ram Sarkar. (2022, March 30). IEEE conference. A fuzzy distance-based ensemble of deep models for cervical cancer detection. 10.1016/j.cmpb.2022.106776

[8] Kaiming He, Xiangyu Zhang, Shaoqing Ren, & Jian Sun. (2016). IEEE conference. Deep Residual Learning for Image Recognition.

[9] J. Kennedy, & R. Eberhart. (n.d.). International Conference on Neural Networks. Particle swarm optimization.

[10] Weixiang Chen, Xiaoyu Han, Jian Wang, Yukun Cao, Xi Jia, Yuting Zheng, Jie Zhou, Wenjuan Zeng, , Lin Wang, Heshui Shi, & Jianjiang Feng. (2022, February). ELSEVIER. Deep diagnostic agent forest (DDAF): A deep learning pathogen recognition system for pneumonia based on CT.

[11] R. Guha, M. Ghosh, P.K. Singh, R. Sarkar, M. Nasipuri, A Hybrid Swarm and Gravitation-based feature selection algorithm for handwritten Indic script classification problem, Complex Intell. Syst. 7 (2) (2021) 823–839.

[12] Bhatt, H., & Shah, M. (2023). A Convolutional Neural Network ensemble model for Pneumonia Detection using chest X-ray images. Healthcare Analytics, 3, 100176. https://doi.org/10.1016/j.health.2023.100176

[13] Sharma, S., & Guleria, K. (2023). A Deep Learning based model for the Detection of Pneumonia from Chest X-Ray Images using VGG-16 and Neural Networks. Procedia Computer Science, 218, 357–366. https://doi.org/10.1016/j.procs.2023.01.018

[14] Zhang, J., Xie, Y., Pang, G., Liao, Z., Verjans, J., Li, W., Sun, Z., He, J., Li, Y., Shen, C., & Xia, Y. (2021). Viral Pneumonia Screening on Chest X-Rays Using Confidence-Aware Anomaly Detection. IEEE Transactions on Medical Imaging, 40(3), 879–890. https://doi.org/10.1109/tmi.2020.3040950